

A peer-reviewed version of this preprint was published in PeerJ on 17 September 2018.

[View the peer-reviewed version](https://peerj.com/articles/5620) (peerj.com/articles/5620), which is the preferred citable publication unless you specifically need to cite this preprint.

Levitskii S, Derbikova K, Baleva MV, Kuzmenko A, Golovin AV, Chicherin I, Krasheninnikov IA, Kamenski P. 2018. 60S dynamic state of bacterial ribosome is fixed by yeast mitochondrial initiation factor 3. PeerJ 6:e5620 <https://doi.org/10.7717/peerj.5620>

An intermediate state of bacterial ribosome dissociation is fixed by yeast mitochondrial initiation factor 3

Sergey Levitskii¹, Ksenia Derbikova¹, Andrey V Golovin^{2,3,4}, Anton Kuzmenko¹, Maria V Baleva¹, Ivan Chicherin¹, Igor A Krasheninnikov¹, Piotr Kamenski^{Corresp. 1,5}

¹ Faculty of Biology, Moscow State University, Moscow, Russia

² Faculty of Bioengineering and Bioinformatics, Moscow State University, Moscow, Russia

³ Institute of Molecular Medicine, Sechenov First Moscow State Medical University, Moscow, Russia

⁴ Faculty of Computer Science, Higher School of Economics, Moscow, Russia

⁵ Institute of Living Systems, I.Kant Baltic Federal University, Kaliningrad, Russia

Corresponding Author: Piotr Kamenski

Email address: peter@protein.bio.msu.ru

The processes of association and dissociation of ribosomal subunits are of great importance for the protein biosynthesis. The mechanistic details of these processes, however, are not well known. In bacteria, upon translation termination, ribosome dissociates into subunits which is necessary for its further involvement into new initiation step. The dissociated state of ribosome is maintained by initiation factor 3 (IF3) which binds to free small subunits and prevents their premature association with the large subunits. In this work, we have exchanged IF3 in *E.coli* cells by its ortholog from *Saccharomyces cerevisiae* mitochondria (Aim23p) and showed that yeast protein cannot functionally substitute the bacterial one and is even slightly toxic for bacterial cells. Our *in vitro* experiments have demonstrated that Aim23p does not split *E.coli* ribosomes into subunits. Instead, it fixes an intermediate state of ribosomes dissociation characterized by sedimentation coefficient about 60S. Using molecular modeling, we show that such fixation is due to mitochondria-specific terminal extensions of Aim23p that stabilize the position of the protein on the bacterial ribosome.

1 **An intermediate state of bacterial ribosome dissociation is fixed by yeast**
2 **mitochondrial initiation factor 3**

3

4 Sergey Levitskii¹, Ksenia Derbikova¹, Andrey V. Golovin^{2,3,4}, Anton Kuzmenko¹, Maria
5 Baleva¹, Ivan Chicherin¹, Igor A. Krasheninnikov¹, Piotr Kamenski^{1*}

6

7 ¹ Faculty of Biology, M.V.Lomonosov Moscow State University, 1/12 Leninskie Gory,
8 Moscow 119234, Russia

9 ² Faculty of Bioengineering and Bioinformatics, M.V.Lomonosov Moscow State
10 University, 1/73 Leninskie Gory, Moscow 119234, Russia

11 ³ Sechenov First Moscow State Medical University, Institute of Molecular Medicine, 8-2
12 Trubetskaya str., Moscow 119991, Russia

13 ⁴ Higher School of Economics, Faculty of Computer Science, 3 Kochnovsky pr., Moscow
14 125319, Russia.

15

16

17 Present address:

18 Anton Kuzmenko, Institute of Molecular Genetics, Russian Academy of Science,
19 Moscow 123182, Russia.

20

21 *Corresponding author: Piotr Kamenski. E-mail: peter@protein.bio.msu.ru

23 ABSTRACT

24 The processes of association and dissociation of ribosomal subunits are of great
25 importance for the protein biosynthesis. The mechanistic details of these processes, however, are
26 not well known. In bacteria, upon translation termination, ribosome dissociates into subunits
27 which is necessary for its further involvement into new initiation step. The dissociated state of
28 ribosome is maintained by initiation factor 3 (IF3) which binds to free small subunits and
29 prevents their premature association with the large subunits. In this work, we have exchanged
30 IF3 in *E.coli* cells by its ortholog from *Saccharomyces cerevisiae* mitochondria (Aim23p) and
31 showed that yeast protein cannot functionally substitute the bacterial one and is even slightly
32 toxic for bacterial cells. Our *in vitro* experiments have demonstrated that Aim23p does not split
33 *E.coli* ribosomes into subunits. Instead, it fixes an intermediate state of ribosomes dissociation
34 characterized by sedimentation coefficient about 60S. Using molecular modeling, we show that
35 such fixation is due to mitochondria-specific terminal extensions of Aim23p that stabilize the
36 position of the protein on the bacterial ribosome.

37

38 INTRODUCTION

39

40 Upon termination of protein biosynthesis in bacteria, 70S ribosome dissociates into small
41 (30S) and large (50S) subunits. Free small subunit then takes part in *de novo* formation of the
42 initiation complex with mRNA, initiator tRNA, and several initiation factors. Binding of the
43 large subunit promotes release of the initiation factors, and associated 70S ribosomes begins a
44 new round of translation (for review, see (Laursen et al. 2005)).

45 The ribosome dissociation / association is, thus, of great importance for the whole process
46 of translation. It is known that bacterial ribosomes dissociate into subunits when the translation
47 termination stage is over; two proteins, namely RRF and EF-G, are responsible for this (Zavialov
48 et al. 2005) (Peske et al. 2005). Once free 30S and 50S subunits appear, initiation factor 3 (IF3)
49 binds to the small subunit in order to keep it apart from the large one (Zavialov et al. 2005). This
50 stage is, in fact, the very first stage of the translation initiation process; 30S•IF3 complex
51 becomes the basis for the full-size initiatory complex formation which includes Shine-Dalgarno
52 sequence of mRNA, initiator tRNA, and initiation factors 1 and 2. It is worth mentioning that
53 anti-association activity of IF3 is definitely of passive mode: it does not promote dissociation of

54 the ribosome into subunits but instead binds to free small subunit and prevents its re-association
55 with the large one (Gualerzi et al. 1977) (Gottlieb et al. 1975).

56 The exact mechanism of ribosome dissociation into subunits remains not clear. This is
57 due to methodological complications of studying this fast and dynamic process. In kinetic study,
58 a model was proposed that assumed the existence of several consecutive conformations of 70S
59 ribosome in course of its dissociation; IF3 was hypothesized to be a potential effector of
60 corresponding conformational changes which could shift the equilibria between different states
61 of dissociating ribosome (Goss et al. 1980). It can be assumed that these conformations might be
62 characterized by different sedimentation coefficients, less than 70S but probably more than 50S.
63 Indeed, a ribosomal ~60S state was described in *in vitro* experiments; this state was formed
64 under specific experimental conditions (Morimoto 1969). The authors used a term “60S
65 component” and postulated that this was a new stable intermediate of the subunits dissociation /
66 association reaction and that this intermediate was just “swollen 70S” (Morimoto 1969). Further
67 investigations, however, have demonstrated that the exact sedimentation coefficient of this
68 “swollen 70S” depends on the sedimentation speed and on the initial 70S concentration (Spirin
69 1971). These results fit very well with the above-discussed hypothesis about consecutive
70 conformational changes of 70S ribosome during dissociation. However, none of these
71 intermediate states has been seen as stable structure.

72 In this work, we investigated the effects of yeast mitochondrial IF3, Aim23p, on the
73 *E.coli* translation. The idea comes from the recent work of Ayyub and colleagues where it has
74 been demonstrated that mammalian mitochondrial IF3 (mtIF3), although being unable to fully
75 substitute for IF3 in *E.coli*, exhibits some functional activity in bacterial cells (Ayyub et al.
76 2018). We exchanged *infC* gene (coding for IF3) in bacteria by AIM23 gene and found that
77 Aim23p cannot substitute the cognate factor. Moreover, Aim23p was slightly toxic for the
78 bacterial cell which was mediated by mitochondria-specific parts of the protein, namely its N-
79 and C-terminal extensions. Our *in vitro* investigations have revealed that Aim23p does bind to
80 *E.coli* ribosome and fixes its unusual state with sedimentation coefficient about 60S. This state
81 can be further transformed into fully dissociated state if Am23p concentration is increased.
82 Terminal extensions of Aim23p have been shown to be responsible for 60S state fixation. Thus,
83 an intermediate state of bacterial ribosome dissociation has been for the first time detected as a
84 stable structure.

85

86 **MATERIALS AND METHODS**

87

88 **Plasmids, *E.coli* strains and oligonucleotides** used in the work may be found in Tables
89 1, 2, and 3, respectively.

90

91 **Cloning and standard procedures**

92 Different versions of AIM23 (*S.cerevisiae*) and *infC* (*E.coli*) genes were cloned into
93 above-mentioned vectors by standard PCR-restriction-ligation approach.

94 Western-blot was performed by standard protocol using the rabbit antibodies against 6-
95 His-tagged recombinant Aim23p (produced on our order by Almabion).

96

97 **Construction of mutant *E.coli* strains (Thomason et al. 2007)**

98 Genomic disruption of *infC* gene coding for IF3 was carried out in the *E.coli* strain
99 MG1655. Cassette for *infC* genomic disruption containing the chloramphenicol resistance gene
100 was prepared by PCR from pKD3 plasmid. Primers (see Table S3) contained 5'-parts designed
101 for the homologous recombination into the target genome site. The cassette was then delivered
102 into *E.coli* cells by electroporation. These cells initially contained pKD46 plasmid encoding for
103 recombinase, as well as pACDH plasmid containing *infC* gene. Clones where recombination
104 took place were selected on chloramphenicol-containing medium and screened by PCR.

105 For transferring the bacterial genetic material to phage P1, 5ml of *E.coli* culture in
106 logarithmic growth phase was infected by 100 ul of phage suspension. The mixture was
107 incubated at 37 °C for 3 hours with shaking and centrifuged at 9200 g for 10 minutes. The phage-
108 containing upper fraction was taken and filtered through 0.45 um filter.

109 For generation of the experimental *E.coli* strains, the MG1655 cells containing pBAD
110 plasmid with cloned *infC* gene were transformed by the plasmids coding for IF3 or different
111 variants of Aim23p. 2 ml of ON cultures were pelleted and resuspended in 1 ml of 10 mM CaCl₂,
112 5mM MgSO₄. Suspensions were 100 ul aliquoted, then half a volume of P1 lysate was added,
113 and the mixtures were incubated at 37 °C for 30 minutes without shaking. Then 1 ml of LB
114 medium and 200 ul of sodium citrate were added followed by the incubation at 37 °C for 1 hour

115 with shaking. The cells were plated on the agar dishes with antibiotics, 0,02% arabinose and
116 5mM sodium citrate. Screening of the clones was performed by PCR.

117 The growth curves of *E.coli* strains were registered in automatic mode using microplate
118 reader Infinite M200 PRO (Tecan Instruments).

119

120 **Ribosome purification and analysis**

121 Ribosomes were isolated from *E.coli* strain MG1655 according to (Rivera et al. 2015)
122 with minor changes. Briefly, bacterial cells from 1L culture with $OD_{600} \sim 0.6$ were collected,
123 lysed, ribosomes from clarified lysate were sedimentated through 10% sucrose cushion, and
124 dissolved in minimal volume of 10 mM Tris-HCl pH 7,0; 60 mM KCl, 60 mM NH_4Cl , 7 mM
125 magnesium acetate, 7 mM β -mercaptoethanol, 0.25 mM EDTA. Isolated ribosomes were stored
126 at $-80^\circ C$. For dissociation reaction, approximately 24 pmoles (one unit of OD_{260}) of ribosomes
127 were mixed with different amounts of recombinant Aim23p, IF3, or Aim23 $\Delta N\Delta C$ in the above-
128 indicated buffer. Mixtures were incubated at $37^\circ C$ for 30 min, and then applied on 15% - 40%
129 continuous sucrose gradients prepared on the same buffer. Samples were centrifuged for 18
130 hours at 100,000 g, and then fractionated from top to bottom (45 fractions each of 250 ul were
131 taken). Absorbencies of all fractions at 260 nm were measured.

132

133 **Molecular modeling**

134 Homology model of Aim23p complex with *E.coli* 30S subunit was done with Modeller
135 9.17 (Sali & Blundell 1993) (script may be found in Supplementary Information). For building of
136 this model, we have used known structure of bacterial 30S subunit complex with the cognate IF3
137 (Pioletti et al. 2001), as well as sequence alignment of Aim23p with *E.coli* IF3 and other
138 orthologs (Atkinson et al. 2012).

139 Folding of Aim23p N-terminal extension was done with AbinitioFold protocol (Bonneau
140 et al. 2002) (Bonneau et al. 2001) on base of fragments obtained from Robetta web server (Kim
141 et al. 2004). Simulation was stopped after 180000 decoys were collected. Homology modeling
142 with new conformation of N-terminal extension was done with Modeller 9.17 (Sali & Blundell
143 1993). Conformation of the C-terminal extension was equilibrated with FloppyTail protocol from
144 Rosetta (Kleiger et al. 2009). Spatial structure visualization was done with the PyMOL
145 Molecular Graphics System, Version 2.0 (Schrödinger, LLC).

146

147 **RESULTS**

148

149 **Full-length Aim23p is undesirable for *E.coli* cells due to its terminal extensions.**

150 As it has been already mentioned in Introduction, mammalian mtIF3 possesses some
151 functional activity in *E.coli* cells (Ayyub et al. 2018). On the other hand, we have previously
152 demonstrated that *E.coli* IF3 may partially rescue the growth defects of the yeast strain lacking
153 Aim23p (Kuzmenko et al. 2014). Moreover, Aim23p was shown to bind to small subunit of
154 bacterial ribosome *in vitro* (Atkinson et al. 2012). Taken together, these findings have allowed us
155 to hypothesize that Aim23p might be at least partially functional in *E.coli* cells as initiation
156 factor 3.

157 To verify this hypothesis, we have constructed three plasmids for further delivery into
158 *E.coli* cells, coding for either cognate IF3 (positive control), Aim23p, or Aim23p without its
159 mitochondria-specific N- and C-terminal extensions (Aim23 Δ N Δ C). This last construct was
160 designed in order to specifically check possible effects of Aim23p terminal extensions on
161 bacterial translation: theoretically, these protein parts, being mitochondria-specific, might not be
162 needed for protein biosynthesis in *E.coli*. Cloned genes of Aim23p and Aim23 Δ N Δ C did not
163 contain sequences coding for mitochondrial targeting sequence. Thereafter, we have disrupted
164 *E.coli infC* gene coding for IF3. This gene contains the promoter for the expression of the
165 downstream gene (Wertheimer et al. 1988), so we have removed only first 153 nucleotides of
166 *infC* gene from the bacterial genome. Since IF3 is indispensable for bacteria, before disruption
167 we have transformed *E.coli* with the plasmid bearing *infC* gene under control of glucose-
168 repressible promoter. Finally, we have delivered the above-described plasmids into bacterial
169 cells and disrupted the genomic copy of *infC* gene. The scheme of bacterial strains engineering is
170 presented on Fig. 1A.

171 Then, we down-regulated the expression of *infC* gene in these strains with glucose and
172 measured their growth rates. The resulting curves may be found in Fig. 1B. The strain bearing
173 wild-type *infC* gene on the plasmid grows normally, with entering the logarithmic phase fast and
174 reaching the plateau. The strain carrying the empty vector shows no growth at first 10 hours of
175 incubation which is easily explained by the absence of *infC* gene. However, slow growth has
176 been detected afterwards, probably as a result of the leakage of glucose-repressed promoter

177 which, in turn, allows minimal amount of IF3 to be synthesized. If *E.coli* cells contain
178 Aim23 Δ N Δ C, the corresponding strain's growth curve is almost identical to that of the strain
179 containing an empty vector. This clearly indicated the impossibility of Aim23 Δ N Δ C to
180 functionally substitute IF3 in bacterial cells. The most interesting case is definitely the bacterial
181 strain bearing the full-size Aim23p. This strain, although reaching finally the level of the strain
182 containing an empty vector, grows measurably slower than strain containing an empty vector.
183 This means that the full-size Aim23p, but not Aim23 Δ N Δ C, negatively affects the viability of
184 *E.coli* cells. It is rather possible that the terminal extensions of Aim23p may somehow interrupt
185 the bacterial translation.

186

187 **Terminal extensions provide the ability of Aim23p to fix an intermediate form of**
188 ***E.coli* ribosomes during dissociation.**

189 The above-described unusual effect of Aim23p in *E.coli* cells has led us to study the
190 interaction of Aim23p with *E.coli* ribosomes *in vitro*. It is well known that adding cognate IF3 to
191 purified bacterial ribosomes shifts the equilibrium of the ribosome dissociation reaction making
192 the dissociated state preferable (Gottlieb et al. 1975). Based on this, we have purified the
193 ribosomes from *E.coli* cells, incubated them with the recombinant IF3 (positive control), or
194 Aim23p, or Aim23 Δ N Δ C, fractionated the reactions by sucrose gradient centrifugation and
195 analyzed the corresponding sedimentation profiles by measuring the optical densities of the
196 fractions at 260 nm. The results of our experiment are presented in Fig. 2A. First of all, the
197 sedimentation of the ribosome sample with no proteins added was characterized by clear UV
198 peaks of 30S and 50S subunits, as well as the whole 70S ribosomes, with the latter being most
199 pronounced. Adding IF3, as expected, led to the complete dissociation of ribosomes into the
200 subunits (disappearance of the 70S peak and significant increase of the 30S and 50S peaks) while
201 adding of Aim23 Δ N Δ C gave no effect on the sedimentation profile. This was also expected: in
202 our *in vivo* experiments, this protein could not substitute for the cognate IF3 in *E.coli* cells (see
203 Fig.1). This seems to be mediated by the impossibility of Aim23 Δ N Δ C to bind the bacterial
204 ribosomes. The profile of sedimentation has been curiously changed with adding the full-size
205 Aim23p. This protein caused a fusion of 50S and 70S peaks with the formation of a single wide
206 and poorly-resolved peak with maximum UV absorbance corresponded to approximately 60S
207 sedimentation coefficient, exactly between 70S and 50S. At the same time, the 30S peak was

208 increased, but to the less extent than in case of the full dissociation promoted by IF3. Since
209 adding of any protein might not increase the sedimentation coefficient of 50S subunit, we have to
210 hypothesize that Aim23p somehow affects the whole ribosome leading to a slight decrease of its
211 buoyant density. The most logical explanation of this phenomenon would be that Aim23p cannot
212 promote the normal ribosome dissociation at concentrations used in the experiment (20:1 molar
213 ratio in relation to the ribosomes concentration) but instead binds to it and fixes an intermediate
214 dissociation state. This state might be less stable than usual ribosome, which should lead to its
215 spontaneous partial dissociation. This is exactly what results from the above-mentioned
216 observation that 30S peak is slightly increased with adding Aim23p. Speaking about the peak of
217 dissociated 50S subunits, it seems to partially overlap with the peak of the “60S intermediate”
218 and thus may not be clearly observed. The appearance of this “60S state” might be the reason of
219 the Aim23p slight toxicity for *E.coli* cells observed by us (see Fig. 1B). It should be noted,
220 finally, that such action of Aim23p on the bacterial ribosomes is definitely mediated by its
221 mitochondria-specific terminal extensions.

222 After obtaining these intriguing results, we have decided to analyze the dose-dependency
223 of the Aim23p effect on *E.coli* ribosomes. The resulting profiles of ribosomes sedimentation
224 after adding Aim23p at different concentrations are presented at Fig. 2B. If Aim23p
225 concentration is 2.5 times more than in previously described experiment (50:1 molar ratio in
226 relation to the ribosomes concentration), then the peak of “60S state” is almost not observed.
227 Instead, one can see a normal 50S peak which is slightly moved towards the increase of the
228 sedimentation coefficient. Probably, Aim23p at this concentration causes almost complete
229 dissociation of the ribosome with just trace amount of “60S state”, which results in minimal shift
230 of the corresponding peak. At the same time, the 30S peak is meaningfully increased relative to
231 the situation when the “60S state” is clearly observed. When Aim23p concentration is increased
232 twice more (up to 100:1 molar ratio in relation to the ribosomes concentration), the resulting
233 profile is identical to that in case of IF3 adding to ribosomes. Summarizing these results, one can
234 conclude that Aim23p in large concentrations does not fix the “60S state” of isolated *E.coli*
235 ribosomes but instead promotes their dissociation into the subunits, like cognate IF3.

236

237 **Aim23p and *E.coli* IF3 act jointly to dissociate bacterial ribosomes *in vitro*.**

238 As it has been mentioned above, the discovered “60S state” of bacterial ribosomes might
239 be the result of the decreased ribosome stability. In other words, the equilibrium of the
240 dissociation reaction in this case may be slightly shifted towards free subunits without full
241 dissociation. This, in turn, means that such state of the ribosome should be subjected to
242 dissociation easier than the normal 70S state. In order to check this hypothesis, we performed *in*
243 *vitro* dissociation experiments with Aim23p and IF3 being simultaneously added to ribosomes.
244 While Aim23p was added in concentration sufficient for “60S state” fixation (10:1 molar ratio in
245 relation to the ribosomes concentration; see Fig. 2C), the amount of IF3 used was not enough for
246 full ribosome dissociation (10:1 molar ratio in relation to the ribosomes concentration). If both
247 proteins were presented in the reaction together (each at the same concentration as alone), the
248 complete dissociation was detected. The only possible explanation of this phenomenon is that
249 “60S state” is indeed subjected to dissociation easier than the normal 70S state. If such
250 intermediate state appears as a result of Aim23p action, the minimal amount of the free 30S
251 subunits is immediately formed (this was also seen in our previous experiments, see Fig. 2A and
252 B). Adding a little amount of the cognate IF3 leads to the fixation of the 30S subunits in their
253 free state and further shifts the reaction equilibrium towards the dissociated state of the
254 ribosome. Thus, Aim23p and IF3 may act jointly to promote the dissociation of the bacterial
255 ribosomes. To verify this, we performed a Western-blot analysis of the ribosomes fractions
256 corresponding to the free subunits and to the whole ribosomes in presence of Aim23p, or IF3, or
257 both proteins together. The results are presented at Fig. 2D. We used the home-made antibodies
258 against 6-His-tagged recombinant Aim23p, and, luckily, they had a significant cross-reactivity
259 with the 6-His-tag (data not shown). Thus, we were able to detect both Aim23p and IF3 in a
260 single sample since IF3 used in our experiments was also 6-His-tagged. As a control, we have
261 used Aim23 Δ N Δ C which, as we have shown before, does not promote any change in *E. coli*
262 ribosomes sedimentation profile. Indeed, we have not detected this truncated protein neither in
263 30S, nor in 70S fractions which means that Aim23 Δ N Δ C is not able to bind the *E. coli* ribosomes.
264 The possibility that our antibodies do not recognize this truncated Aim23p version can be
265 excluded since this protein has been detected by the same antibodies in the yeast cells (data not
266 shown). IF3 in this experiment has been found to bind exclusively free 30S subunits but not 70S
267 ribosomes, exactly as expected. Aim23p, however, is detected both in free 30S subunits and in
268 the 70S ribosomes fractions, and this does not qualitatively depend on presence or absence of IF3

269 in the reaction. This explains well the joint action of these two proteins resulting in the
270 ribosomes dissociation which cannot be achieved when using Aim23p and IF3 at the same
271 concentrations separately.

272

273 **Terminal extensions of Aim23p ensure protein interaction with *E.coli* ribosomes by** 274 **fixing Aim23p core part on the small subunit**

275 A very interesting question rises from the above-described results: in which manner does
276 Aim23p interact with bacterial ribosome and what is the role of its terminal extensions in such
277 interaction? To answer this question, we have performed molecular modeling.

278 Previously (Atkinson et al. 2012) sequence alignment of Aim23p with *E.coli* IF3 and
279 other orthologs has been done. On the base of this data, as well as the known structure of 30S
280 complex with the cognate IF3 (Pioletti et al. 2001), we have built the homology model of
281 Aim23p complex with *E.coli* 30S ribosomal subunit with the help of Modeller 9.18 (script may
282 be found in Supplementary Information). Resulting structure eventually has a long and extended
283 N-terminal tail (Suppl. Fig.2). Size of this tail was comparable with size of 30S subunit and
284 model could not provide valuable information about N-terminal extension function. We have
285 suggested that N-terminal extension is somehow structured and have built the corresponding
286 model with Rosetta AbInitio protocol. From 18398 decoys of N-terminal extension, top ten had
287 alpha helical structure with RMSD less than 10 Å. This observation reflects the fact that N-
288 terminal extension does not possess certain spatial structure but probably has mobile helical
289 packaging. N-terminal extension model with best Rosetta score was used to rebuild new
290 homology model of 16S RNA and Aim23p complex. Resulting model has surprisingly revealed
291 strong interaction of N-terminal extension with C-terminal domain of Aim23p core part and with
292 long 3' terminal helix of 16S RNA. Additional distance restraints between centers of mass from
293 15 to 40 Å were applied to sample distance between Aim23p's N-terminal extension and C-
294 terminal domain. As a result, top models have confirmed interaction of N-terminal extension
295 with C-terminal domain, while interaction with 16S RNA does not look favorable. Best models
296 of packed C-terminal extension showed interaction with N-terminal domain. The summary of
297 molecular modeling is presented in Figure 3.

298

299 **DISCUSSION**

300 We have demonstrated previously that *E.coli* IF3 fused with the mitochondrial targeting
301 sequence of Aim23p may complement to minimal extent the absence of AIM23 gene in yeast
302 (Kuzmenko et al. 2014) which is a strong evidence of Aim23p being *bona fide* initiation factor 3
303 in mitochondria. This finding is not surprising taking into account that bacterial enzymes can
304 often functionally substitute for their mitochondrial orthologues. This, for example, has been
305 demonstrated for several aminoacyl-tRNA synthetases (Edwards & Schimmel 1987) (Chiu et al.
306 2009) and for the proteins involved in Fe-S clusters formation (Kispal et al. 1999). In this work,
307 we have performed “reverse” experiment and investigated if Aim23p is able to substitute for
308 cognate IF3 in *E.coli* cells. The cases of successful complementation of bacterial proteins by
309 their mitochondrial orthologues have been described remarkably rarer than the opposite
310 situations. However, mammalian mitochondrial initiation factor 2 has been shown to function in
311 *E.coli* cells instead of two cognate factors at once, namely IF1 and IF2 (Gaur et al. 2008). Most
312 probably, this is due to the short insertion domain of mammalian mtIF2 that is believed to
313 execute the function of IF1 in mitochondria. Moreover, in a recent work it has been
314 demonstrated that mammalian mtIF3, although not being able to fully substitute for IF3 in *E.coli*,
315 exhibits some functional activity in bacterial cells (Ayyub et al. 2018). Speaking about Aim23p,
316 this protein, as we have discovered in the present study, does not work as an initiation factor in
317 *E.coli*, independently of presence or absence of the terminal extensions. We used an
318 experimental system where cognate IF3 gene was disrupted in the bacterial genome but was
319 presented on the plasmid under the control of glucose-repressible promoter. Such promoters are
320 well known to leak if the amount of glucose is low. In our case, this allows the synthesis of
321 minimal amount of IF3 and weak growth of the bacterial culture after a dozen of hours of
322 incubation, when the main portion of glucose becomes utilized by bacterial cells (Fig. 1B).
323 Surprisingly, this weak growth is even slower in presence of full-size Aim23p when comparing
324 to Aim23p without terminal extensions. This means that these regions of Aim23p even make this
325 protein slightly toxic for bacterial cells. Interestingly, mammalian mtIF3 behaves quite
326 differently in *E.coli*. Full-size factor does not markedly affect the *E.coli* growth rate while
327 deletion of the N-terminal extension leads to the severe growth impairment (Ayyub et al. 2018).
328 However, to our opinion, these results should not be directly compared with the data presented in
329 this work. The main reason for this is the difference in the experimental systems. Ayyub and
330 colleagues used the mutant strain in which IF3 was devoid of first 55 amino acids and was

331 synthesized in normal quantities. Earlier, the same authors have shown that this truncated version
332 of IF3 is enough for *E.coli* survival and can perform all main functions of the factor (Ayyub et al.
333 2017). This means that the action of any mtIF3 version in such cells is somewhat additional to
334 the action of the cognate factor. On the contrary, our *E.coli* cells contained minimal amount of
335 wild-type IF3 synthesized from repressed but leaking promoter, and the quantity of Aim23p
336 encoded in the plasmid was much higher. In this case, the heterologous factor influence on the
337 bacterial cells might be stronger than that discovered by Ayyub and colleagues.

338 The negative influence of Aim23p on *E.coli* cells, most probably, might realize *via* its
339 interaction with bacterial ribosomes. This is exactly what we have demonstrated in the present
340 work. In certain concentration range, Aim23p promotes the formation of a very unusual state of
341 *E.coli* ribosomes *in vitro*. Our results presented in Fig.2 indicate that this state is characterized by
342 the partial fusion of 70S and 50S peaks. The maximum of absorbance at 260 nm in this case
343 approximately corresponds to the 60S sedimentation coefficient. We propose to call it “60S
344 intermediate dissociation state”. To our current knowledge, such ribosome state has never been
345 detected *in vivo*. However, it was described in *in vitro* experiments (Morimoto 1969), notably at
346 approximately the same magnesium concentrations as we used in our work (10 mM vs 7 mM,
347 respectively). Morimoto used a term “60S component” and postulated that this was a new stable
348 intermediate of the subunits association reaction and that this intermediate was just “swollen
349 70S” (Morimoto 1969). Further investigations, however, have demonstrated that the
350 sedimentation coefficient of this “swollen 70S” depends on the centrifugation speed and on the
351 initial 70S concentration (Spirin 1971). This clearly indicates that discussed ~60S zone on the
352 sedimentation pattern is the consequence of the dynamic equilibrium of dissociation-association
353 reaction rather than the stationary ribosomal structure.

354 In this work, the 60S intermediate dissociation state has been for the very first time fixed
355 by adding a protein to the ribosomes. Aim23p possesses this activity due to its terminal
356 extensions since we have not seen any changes in the ribosome sedimentation profile when
357 adding Aim23 Δ N Δ C (Fig. 2A). This has been confirmed by the molecular modeling of Aim23p
358 complex with 30S: terminal extensions of Aim23p (especially N-terminal one) have been shown
359 to interact directly with the core protein part which probably makes Aim23p “fixed” on the small
360 subunit (see Fig.3). Interestingly, the similar effect of mammalian mtIF3 has been described with
361 regard to human mitochondrial ribosomes dissociation *in vitro* (Haque et al. 2008). Full-length

362 mtIF3 promotes normal dissociation while using its truncated version without terminal
363 extensions causes the partial fusion of the 39S (large subunit) and 55S (whole mitoribosome)
364 peaks. This clearly indicates some abnormal dissociation. Probably, terminal extensions of
365 mitochondrial IF3s prevent the formation of intermediate dissociation states in case of
366 mitoribosomes but promote their formation when acting on the bacterial ribosomes.

367 In the present work, the “60S state” has been demonstrated to dissociate by increased
368 amount of Aim23p (Fig. 2B), or by a small amount of *E.coli* IF3 (Fig. 2C). The slight toxicity of
369 Aim23p for *E.coli* cells (see above, Fig. 1B) may be also explained by fixing the “60S state”
370 which dissociates poorly in presence of marginal IF3 quantities synthesized from leaking
371 promoter. At the same time, the presence of even large amount of Aim23p in *E.coli* cells
372 together with the physiological amount of the cognate IF3 has no effect on bacterial viability, as
373 we could see when purifying recombinant Aim23p from wild-type *E.coli* cells (data not shown).
374 Even if “60S state” is fixed in such conditions, it might rapidly dissociate to the subunits with the
375 help of IF3. This may be also the case in the work of Ayyub and colleagues: having sufficient
376 amounts of cognate *E.coli* IF3 allows bacterial ribosomes to keep the dissociated state *in vivo*
377 properly regardless on the mammalian mtIF3 presence, and this could explain almost normal
378 growth of the corresponding bacterial strains (Ayyub et al. 2018).

379 The question if “60S intermediate state” exists in wild-type bacterial cells is of high
380 interest since it is worth proposing that *in vitro* ribosomes could not pose a conformation which
381 is not pertained to them *in vivo*. The answer “no”, however, seems to be obvious as bacterial IF3
382 is well-known to bind only free 30S subunits. This was also seen in the present work (Fig. 2D).
383 At the same time, IF3 must bind 70S ribosomes, or at least keep bound to 30S when 70S is
384 already formed, to fix any dissociation intermediate. The impossibility of this binding is not
385 dogmatic. In the structural study, IF3 was found as a part of the fully assembled bacterial
386 initiator complex, together with 70S ribosomes (Allen et al. 2005). The authors propose that IF3
387 does bind the free 30S subunit initially and then remains bound to 70S ribosomes for a short time
388 after subunits association. Moreover, in a recent study binding of IF3 with 70S ribosome was
389 confirmed by FRET experiments, and an alternative binding site of IF3 was identified on 50S
390 subunit (Goyal et al. 2017). The subunits association in presence of IF3 might be realized *via*
391 some intermediate states relative to the “60S state” detected in the present work.

392 The possible mechanisms of the *E.coli* ribosomes 60S intermediate state formation and
393 dissociation are summarized in Fig.4.

394

395

396

397 CONCLUSIONS

398 The main result of this work is the detection of an intermediate state of *E.coli* ribosomes
399 dissociation (“60S state”). This state was for the very first time fixed by protein (*S.cerevisiae*
400 mitochondrial translation initiation factor 3, Aim23p). We also demonstrate that Aim23p and
401 cognate *E.coli* IF3 actions on bacterial ribosome are of different modes and that these two
402 proteins may bind it jointly. Using computer modeling, we show that the key players in the game
403 of Aim23p binding to *E.coli* ribosomes are protein’s mitochondria-specific terminal extensions
404 that nestle the core part of Aim23p to ribosomal small subunit. Thus, the binding efficiency
405 increases. Our results provide a basis for future structural studies of “60S state” which, in turn,
406 will elucidate the fine mechanisms of bacterial ribosome dissociation / association.

407

408

409 ACKNOWLEDGEMENTS

410 We are grateful to Gemma Atkinson (Umea University, Sweden, and Tartu University,
411 Estonia) for the *in silico* prediction of Aim23p terminal extensions. We also thank Konstantin
412 Khodosevich (Copenhagen University, Denmark), Vasili Hauryliuk (Umea University, Sweden,
413 and Tartu University, Estonia), Ivan Tarassov (Strasbourg University, France), Stanislav
414 Kozlovsky and Alexey Kharitonov (Moscow University, Russia) for providing strains and
415 chemicals. We appreciate the improvement of the figures quality by Alexey Fedyakov (Moscow
416 University, Russia). Our special thanks are to Sergey Dmitriev (Moscow University, Russia) and
417 to Vyacheslav Kolb (Institute of Protein Research, Russia) and his lab members for helpful
418 discussions. The technical help of our students Maria Klimontova, Valeria Zinina, Anna
419 Mirnaya, Anastasia Kapusta, and Margarita Chudenkova is greatly appreciated.

420

421 REFERENCES

- 422 Allen GS, Zavialov A, Gursky R, Ehrenberg M, and Frank J. 2005. The cryo-EM
423 structure of a translation initiation complex from Escherichia coli. *Cell* 121:703-712. DOI
424 10.1016/j.cell.2005.03.023.
- 425 Atkinson GC, Kuzmenko A, Kamenski P, Vysokikh MY, Lakunina V, Tankov S,
426 Smirnova E, Soosaar A, Tenson T, and Hauryliuk V. 2012. Evolutionary and genetic analyses of
427 mitochondrial translation initiation factors identify the missing mitochondrial IF3 in *S.*
428 *cerevisiae*. *Nucleic Acids Res* 40:6122-6134. DOI 10.1093/nar/gks272
- 429 Ayyub SA, Dobriyal D, and Varshney U. 2017. Contributions of the N- and C-Terminal
430 Domains of Initiation Factor 3 to Its Functions in the Fidelity of Initiation and Antiassociation of
431 the Ribosomal Subunits. *J Bacteriol* 199. DOI 10.1128/JB.00051-17
- 432 Ayyub SA, Dobriyal D, Aluri S, Spremulli LL, and Varshney U. 2018. Fidelity of
433 translation in the presence of mammalian mitochondrial initiation factor 3. *Mitochondrion* 39:1-
434 8. DOI 10.1016/j.mito.2017.08.006
- 435 Bonneau R, Strauss CE, Rohl CA, Chivian D, Bradley P, Malmstrom L, Robertson T, and
436 Baker D. 2002. De novo prediction of three-dimensional structures for major protein families. *J*
437 *Mol Biol* 322:65-78.
- 438 Bonneau R, Tsai J, Ruczinski I, Chivian D, Rohl C, Strauss CE, and Baker D. 2001.
439 Rosetta in CASP4: progress in ab initio protein structure prediction. *Proteins Suppl* 5:119-126.
440 DOI 10.1002/prot.1170
- 441 Chiu WC, Chang CP, and Wang CC. 2009. Evolutionary basis of converting a bacterial
442 tRNA synthetase into a yeast cytoplasmic or mitochondrial enzyme. *J Biol Chem* 284:23954-
443 23960. DOI 10.1074/jbc.M109.031047
- 444 Edwards H, and Schimmel P. 1987. An *E. coli* aminoacyl-tRNA synthetase can substitute
445 for yeast mitochondrial enzyme function in vivo. *Cell* 51:643-649.
- 446 Gaur R, Grasso D, Datta PP, Krishna PD, Das G, Spencer A, Agrawal RK, Spremulli L,
447 and Varshney U. 2008. A single mammalian mitochondrial translation initiation factor
448 functionally replaces two bacterial factors. *Mol Cell* 29:180-190. DOI
449 10.1016/j.molcel.2007.11.021
- 450 Goss DJ, Parkhurst LJ, and Wahba AJ. 1980. Kinetics of ribosome dissociation and
451 subunit association. The role of initiation factor IF3 as an effector. *J Biol Chem* 255:225-229.

- 452 Gottleib M, Davis BD, and Thompson RC. 1975. Mechanism of dissociation of
453 ribosomes of Escherichia coli by initiation factor IF-3. *Proc Natl Acad Sci U S A* 72:4238-4242.
- 454 Goyal A, Belardinelli R, and Rodnina MV. 2017. Non-canonical Binding Site for
455 Bacterial Initiation Factor 3 on the Large Ribosomal Subunit. *Cell Rep* 20:3113-3122. DOI
456 10.1016/j.celrep.2017.09.012
- 457 Gualerzi C, Risuleo G, and Pon CL. 1977. Initial rate kinetic analysis of the mechanism
458 of initiation complex formation and the role of initiation factor IF-3. *Biochemistry* 16:1684-1689.
- 459 Haque ME, Grasso D, and Spremulli LL. 2008. The interaction of mammalian
460 mitochondrial translational initiation factor 3 with ribosomes: evolution of terminal extensions in
461 IF3mt. *Nucleic Acids Res* 36:589-597. DOI 10.1093/nar/gkm1072
- 462 Kim DE, Chivian D, and Baker D. 2004. Protein structure prediction and analysis using
463 the Robetta server. *Nucleic Acids Res* 32:W526-531. DOI 10.1093/nar/gkh468
- 464 Kispal G, Csere P, Prohl C, and Lill R. 1999. The mitochondrial proteins Atm1p and
465 Nfs1p are essential for biogenesis of cytosolic Fe/S proteins. *EMBO J* 18:3981-3989. DOI
466 10.1093/emboj/18.14.3981
- 467 Kleiger G, Saha A, Lewis S, Kuhlman B, and Deshaies RJ. 2009. Rapid E2-E3 assembly
468 and disassembly enable processive ubiquitylation of cullin-RING ubiquitin ligase substrates. *Cell*
469 139:957-968. DOI 10.1016/j.cell.2009.10.030
- 470 Kuzmenko A, Atkinson GC, Levitskii S, Zenkin N, Tenson T, Hauryliuk V, and
471 Kamenski P. 2014. Mitochondrial translation initiation machinery: conservation and
472 diversification. *Biochimie* 100:132-140. DOI 10.1016/j.biochi.2013.07.024
- 473 Laursen BS, Sorensen HP, Mortensen KK, and Sperling-Petersen HU. 2005. Initiation of
474 protein synthesis in bacteria. *Microbiol Mol Biol Rev* 69:101-123. DOI
475 10.1128/MMBR.69.1.101-123.2005
- 476 Morimoto T. 1969. Intermediate stage in the association and dissociation of Escherichia
477 coli ribosomes and the combining properties of their subunits. *Biochim Biophys Acta* 182:135-
478 146.
- 479 Peske F, Rodnina MV, and Wintermeyer W. 2005. Sequence of steps in ribosome
480 recycling as defined by kinetic analysis. *Mol Cell* 18:403-412. DOI
481 10.1016/j.molcel.2005.04.009

482 Pioletti M, Schlunzen F, Harms J, Zarivach R, Gluhmann M, Avila H, Bashan A, Bartels
483 H, Auerbach T, Jacobi C, Hartsch T, Yonath A, and Franceschi F. 2001. Crystal structures of
484 complexes of the small ribosomal subunit with tetracycline, edeine and IF3. *EMBO J* 20:1829-
485 1839. DOI 10.1093/emboj/20.8.1829

486 Rivera MC, Maguire B, and Lake JA. 2015. Isolation of ribosomes and polysomes. *Cold
487 Spring Harb Protoc* 2015:293-299. DOI 10.1101/pdb.prot081331

488 Sali A, and Blundell TL. 1993. Comparative protein modelling by satisfaction of spatial
489 restraints. *J Mol Biol* 234:779-815. DOI 10.1006/jmbi.1993.1626

490 Spirin AS. 1971. On the equilibrium of the association-dissociation reaction of ribosomal
491 subparticles and on the existence of the so-called '60 S intermediate' ('swollen 70 S') during
492 centrifugation of the equilibrium mixture. *FEBS Lett* 14:349-353.

493 Thomason LC, Costantino N, and Court DL. 2007. E. coli genome manipulation by P1
494 transduction. *Curr Protoc Mol Biol* Chapter 1:Unit 1. DOI 10.1002/0471142727.mb0117s79

495 Wertheimer SJ, Klotsky RA, and Schwartz I. 1988. Transcriptional patterns for the thrS-
496 infC-rplT operon of Escherichia coli. *Gene* 63:309-320.

497 Zavialov AV, Haurlyiuk VV, and Ehrenberg M. 2005. Splitting of the posttermination
498 ribosome into subunits by the concerted action of RRF and EF-G. *Mol Cell* 18:675-686. DOI
499 10.1016/j.molcel.2005.05.016

500

501

502 **FIGURE LEGENDS**

503

504 **Fig.1.** Aim23p without terminal extensions is non-functional in *E.coli* cells while full-
505 size Aim23p is even slightly toxic. (A) Scheme of the mutant *E.coli* strains production. At the
506 first stage, the *infC* gene coded for *E.coli* IF3 was cloned into pACDH vector. The resulting
507 plasmid was delivered into *E.coli* cells following by the genomic disruption of *infC* by the
508 chloramphenicol resistance gene (Cat). The *infC* gene on the plasmid made the resulting strain
509 viable. Then, the cells were inoculating by P1 phage in order to capture the genomic DNA region
510 containing the disrupted *infC* gene. The result of the first stage was the phage with the above-
511 mentioned genomic DNA region. On the second stage, the *infC* gene was cloned into pBAD
512 vector (under control of glucose-repressible promoter), and genes of Aim23p and Aim23 Δ N Δ C

513 were cloned into pACDH vector. pBAD-*infC* and pACDH with one of the above-mentioned
514 genes were then delivered into wild-type *E.coli* cells following by the inoculation by the phage
515 from the first stage. This was resulted in the substitution of the wild-type *infC* genomic copy by
516 the disrupted gene. As a result, a series of *E.coli* strains were generated with the following
517 features: (1) genomic disruption of *infC*, (2) presence of *infC* on the pBAD vector, (3) presence
518 of *infC* (positive control), Aim23p, or Aim23 Δ N Δ C on the pACDH vector. **(B)** Growth curves of
519 the *E.coli* strains (indicated on the right) obtained as described in Fig. 3A. Bacteria were initially
520 incubated without glucose, then the medium was changed to the glucose-containing one, and the
521 optical density registration began. Each strain contained *infC* gene on the pBAD vector under
522 control of glucose-repressible promoter. IF3: *infC* gene on the pACDH vector. Vector: empty
523 pACDH. Aim23 and Aim23 Δ N Δ C: full-size and truncated AIM23 genes, respectively, on the
524 pACDH vector.

525

526 **Fig. 2.** The unusual effects of Aim23p on *E.coli* ribosomes *in vitro*. **(A, B, C)** Ribosomes
527 sedimentation profiles: optical densities at 260 nm (Y-axes of the each graph) of different
528 fractions of *E.coli* ribosomes which were pre-incubated with the indicated proteins and
529 sedimentated in the sucrose gradient. On the X-axes: 20-25 sequential fractions, from bottom to
530 top of the gradient. Molar ratios protein:ribosomes are indicated near each sedimentation profile.
531 The peaks corresponded to the ribosomes and their free subunits are marked with the vertical
532 dotted lines and are designated below the graphs. **(D)** Western-blot hybridization of different
533 fractions of *E.coli* ribosomes which were pre-incubated with the indicated proteins and
534 sedimented in the sucrose gradient. In each case, the mixture of 2 fractions composing the peaks
535 of 30S or 70S was analyzed (indicated on the top). Aim23 Δ N Δ C: 2 fractions composing the
536 corresponding peaks on Fig. 2A. All other samples: 2 fractions composing the corresponding
537 peaks on Fig. 2C. We used the antibodies against recombinant Aim23p with the significant
538 cross-reactivity to the 6-His-tag which allowed us to detect both Aim23p and IF3 (indicated by
539 arrows on the left) in the single analysis.

540

541 **Fig. 3.** Model of Aim23p interactions with *E.coli* 16S RNA. N-terminal extension is in
542 light-pink, N-terminal domain is in hot-pink, C-terminal domain is in magenta and C-terminal
543 extension is in deep-purple. 16S RNA is in black and white. **(A)** Overview of Aim23p location

544 on 16S RNA. **(B)** Close-up view in same orientation. **(C)** Close-up view with counterclockwise
545 rotation around vertical axis displaying proximity of N-terminal extension, C-terminal domain
546 and 16S RNA.

547

548 **Fig.4.** The hypothetic scheme of the formation and dissociation of *E.coli* ribosomes
549 intermediate state *in vitro*. 1. Initially, the small (SSU) and large (LSU) subunits of the ribosome
550 are associated one to another (70S). Adding of Aim23p (the terminal extensions are represented
551 by black boxes) changes the ribosome conformation making the subunits more flexible relative
552 to one another and allowing their reciprocal movements without full dissociation (60S). 2. This
553 intermediate dissociation state cannot spontaneously dissociate to the subunits in presence of
554 Aim23p. 3. Adding more Aim23p, however, shifts the dissociation reaction equilibrium which
555 results in appearance of the free SSU and LSU (30S + 50S). 4. Full dissociation of the
556 intermediate can also be reached by adding *E.coli* IF3 in amount insufficient for dissociation of
557 70S ribosomes.

Table 1 (on next page)

Table 1. Plasmids used in this work.

1 **Table 1. Plasmids used in the work**

Plasmid	Description
pACDH	Low-copy vector for expression in <i>E.coli</i>
pACDHinfC*	pACDH with cloned <i>infC</i> gene from <i>E.coli</i>
pACDHAim23*	pACDH with cloned AIM23 gene lacking mitochondrial targeting sequence
pACDHAim23ΔNΔC*	pACDH with cloned AIM23 gene lacking mitochondrial targeting sequence and both terminal extensions
pBAD	Vector for <i>E.coli</i> expression containing glucose-repressible promoter
pBADinfC*	pBAD with cloned <i>infC</i> gene from <i>E.coli</i>
pKD3	Plasmid containing FRT-cat-FRT for preparation of <i>E.coli</i> disruption cassettes
pKD46	Plasmid with Lambda Red recombinase from phage λ for efficient gene disruption in <i>E.coli</i>
pET32a	Vector for the heterologous proteins expression in <i>E.coli</i>
pETIF3*	pET32a with cloned <i>infC</i> gene from <i>E.coli</i>
pETAim23*	pET32a with cloned AIM23 gene lacking mitochondrial targeting sequence
pETAim23ΔNΔC*	pET32a with cloned AIM23 gene lacking mitochondrial targeting sequence and both terminal extensions

2 * Generated in this work.

3

Table 2 (on next page)

Table 2. *E.coli* strains used in this work.

1 **Table 2. *E.coli* strains used in the work**

Strain	Genotype / Description / Purpose
MG 1655	K-12 F ⁻ λ ⁻ ilvG ⁻ rfb-50 rph-1 For genetic manipulations, for ribosome isolation
MG_infC_ACDH*	MG 1655 + pACDHinfC + pKD46
MG_ΔIF3*	MG_infC_ACDH with first 153 nucleotides of <i>inf3</i> gene exchanged by chloramphenicol resistance cassette
MG_infC_BAD* ("vector" on Fig.3)	MG 1655 + pBADinfC + pACDH
MG_IF3* ("IF3" on Fig.3)	MG 1655 + pBADinfC + pACDHinfC
MG_Aim23* ("Aim23" on Fig.3)	MG 1655 + pBADinfC + pACDHAim23
MG_Aim23ΔNΔC* ("Aim23ΔNΔC" on Fig.3)	MG 1655 + pBADinfC + pACDHAim23ΔNΔC
Rosetta (DE3) pLysS	F ⁻ ompT hsdS _B (R _B ⁻ m _B ⁻) gal dcm λ(DE3 [lacI lacUV5-T7 gene 1 ind1 sam7 nin5]) pLysSRARE (Cam ^R) For heterologous proteins synthesis and purification
Top10	F- mcrA Δ(mrr-hsdRMS-mcrBC) φ80lacZΔM15 ΔlacX74 nupG recA1 araD139 Δ(ara-leu)7697 galE15 galK16 rpsL(Str ^R) endA1 λ ⁻ For molecular cloning

2 * Generated in this work.

3

4

Table 3 (on next page)

Table 3. Oligonucleotides used in this work.

1 **Table 3. Oligonucleotides used in the work**

2 (all synthesized by Evrogen)

3 Restriction sites are in capital letters.

1	Cloning of IF3 into pACDH and pBAD	tcagccatggcctaaaggcggaaaacgagttc
2		tcaggaattcctactgtttcttcttaggagcga
3	Cloning of AIM23 Δ N Δ C into pACDH	tcagccatggcctggagcaccgggaca
4		tcaggaattcctatggtttaacgtcctttggta
5	Cloning of AIM23 into pACDH	tcagccatggcctaatgcatcatctaccacag
6		tcaggaattcctacatttcattcatttttttctctg
7	Production of chloramphenicol resistance disruption cassette	tgcaacaagagattcgcagccgcagtcttaacaattggaggaataaggtatgga agaaaaaatcactgg
8		ccattatacgacaaaaccggcgctcggcgtagggctgatctcgactaagtcac gcagtactgttgta
9	Screening of IF3 disruption and transduction (PCR-product is synthesized in case of IF3 gene conservation only)	caggaagttcgcttaacagg
10		ggttagcgtgcttgtgc
11	Screening of IF3 disruption and transduction (PCR-products from IF3 gene and from disruption cassette are different in size)	gacgtaaatgaagtgatcgagaag
12		ggttagcgtgcttgtgc
13	AIM23 cloning into pET32a	gactCATATGaatgcatcatctaccacaga
14		ctagCTCGAGcatttcattcatttttttctct
15	AIM23 Δ N Δ C cloning into pET32a	gactCATATGtggagcaccgggacaga
16		ctagCTCGAGtggtttaacgtcctttggta
17	IF3 cloning into pET32a	atgcCATATGaaaggcggaaaacgagttc
18		actgCTCGAGctgtttcttcttaggagcg
19	Screening of pET32a-based constructs	gctagtattgctcagcgg
20		atgcgtccggcgtaga

4

5

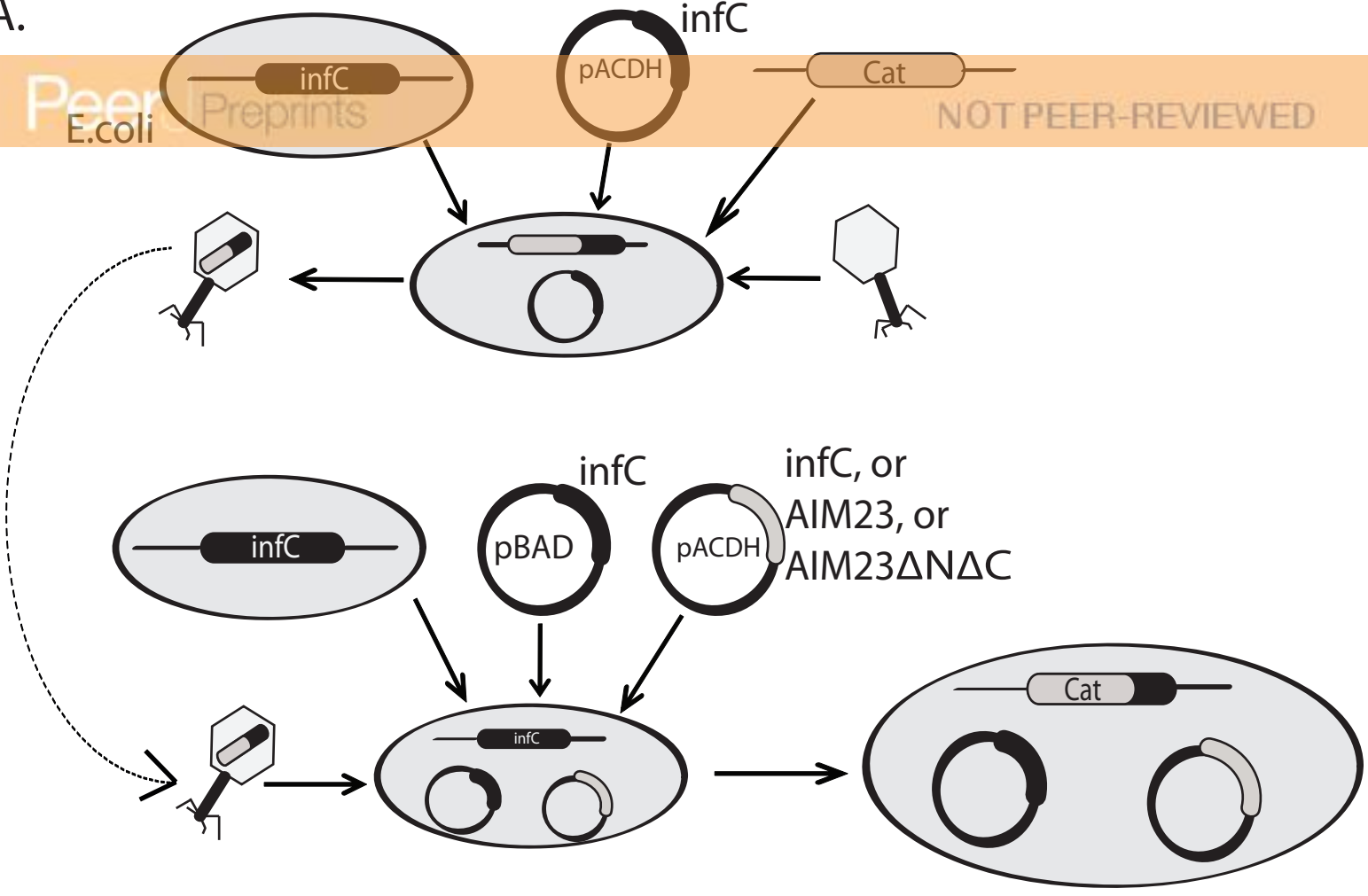
6

Figure 1(on next page)

Aim23p without terminal extensions is non-functional in *E.coli* cells while full-size Aim23p is even slightly toxic.

(A) Scheme of the mutant *E.coli* strains production. At the first stage, the *infC* gene coded for *E.coli* IF3 was cloned into pACDH vector. The resulting plasmid was delivered into *E.coli* cells following by the genomic disruption of *infC* by the chloramphenicol resistance gene (Cat). The *infC* gene on the plasmid made the resulting strain viable. Then, the cells were inoculating by P1 phage in order to capture the genomic DNA region containing the disrupted *infC* gene. The result of the first stage was the phage with the above-mentioned genomic DNA region. On the second stage, the *infC* gene was cloned into pBAD vector (under control of glucose-repressible promoter), and genes of Aim23p and Aim23 Δ N Δ C were cloned into pACDH vector. pBAD-*infC* and pACDH with one of the above-mentioned genes were then delivered into wild-type *E.coli* cells following by the inoculation by the phage from the first stage. This was resulted in the substitution of the wild-type *infC* genomic copy by the disrupted gene. As a result, a series of *E.coli* strains were generated with the following features: (1) genomic disruption of *infC*, (2) presence of *infC* on the pBAD vector, (3) presence of *infC* (positive control), Aim23p, or Aim23 Δ N Δ C on the pACDH vector. **(B)** Growth curves of the *E.coli* strains (indicated on the right) obtained as described in Fig. 3A. Bacteria were initially incubated without glucose, then the medium was changed to the glucose-containing one, and the optical density registration began. Each strain contained *infC* gene on the pBAD vector under control of glucose-repressible promoter. IF3: *infC* gene on the pACDH vector. Vector: empty pACDH. Aim23 and Aim23 Δ N Δ C: full-size and truncated AIM23 genes, respectively, on the pACDH vector.

A.



B.

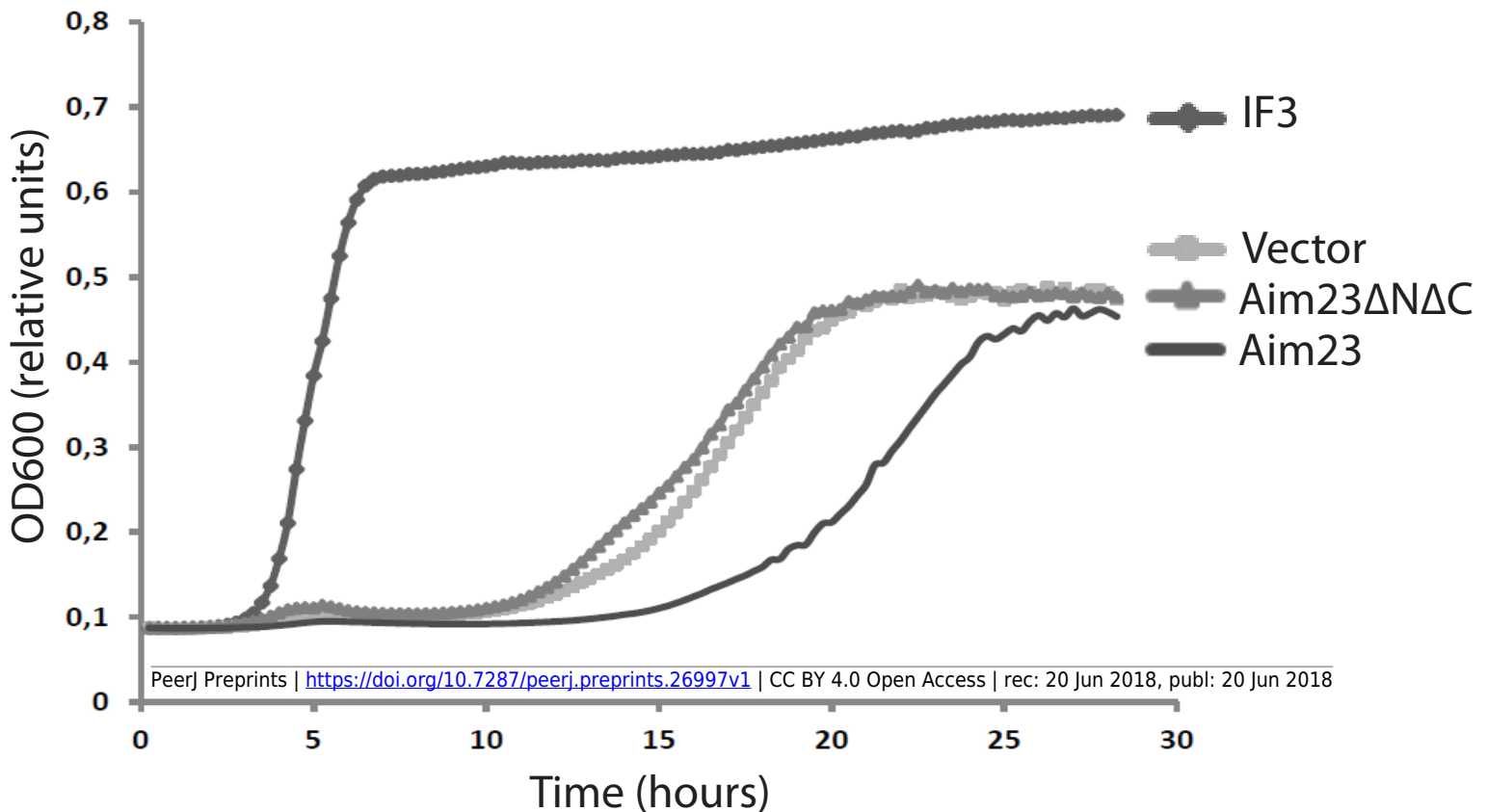
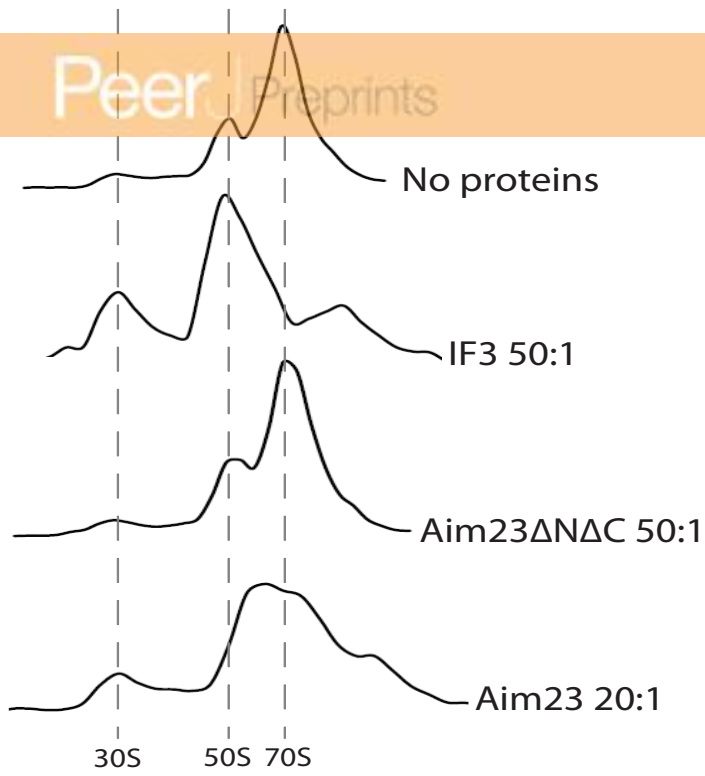


Figure 2 (on next page)

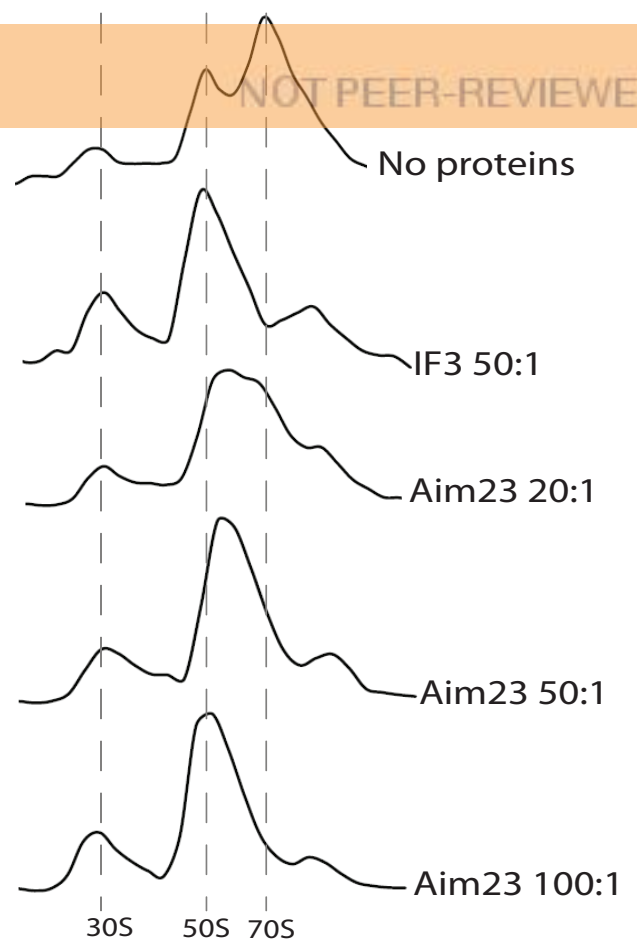
The unusual effects of Aim23p on *E.coli* ribosomes *in vitro*.

(A, B, C) Ribosomes sedimentation profiles: optical densities at 260 nm (Y-axes of the each graph) of different fractions of *E.coli* ribosomes which were pre-incubated with the indicated proteins and sedimentated in the sucrose gradient. On the X-axes: 20-25 sequential fractions, from bottom to top of the gradient. Molar ratios protein:ribosomes are indicated near each sedimentation profile. The peaks corresponded to the ribosomes and their free subunits are marked with the vertical dotted lines and are designated below the graphs. **(D)** Western-blot hybridization of different fractions of *E.coli* ribosomes which were pre-incubated with the indicated proteins and sedimented in the sucrose gradient. In each case, the mixture of 2 fractions composing the peaks of 30S or 70S was analyzed (indicated on the top). Aim23 Δ N Δ C: 2 fractions composing the corresponding peaks on Fig. 2A. All other samples: 2 fractions composing the corresponding peaks on Fig. 2C. We used the antibodies against recombinant Aim23p with the significant cross-reactivity to the 6-His-tag which allowed us to detect both Aim23p and IF3 (indicated by arrows on the left) in the single analysis.

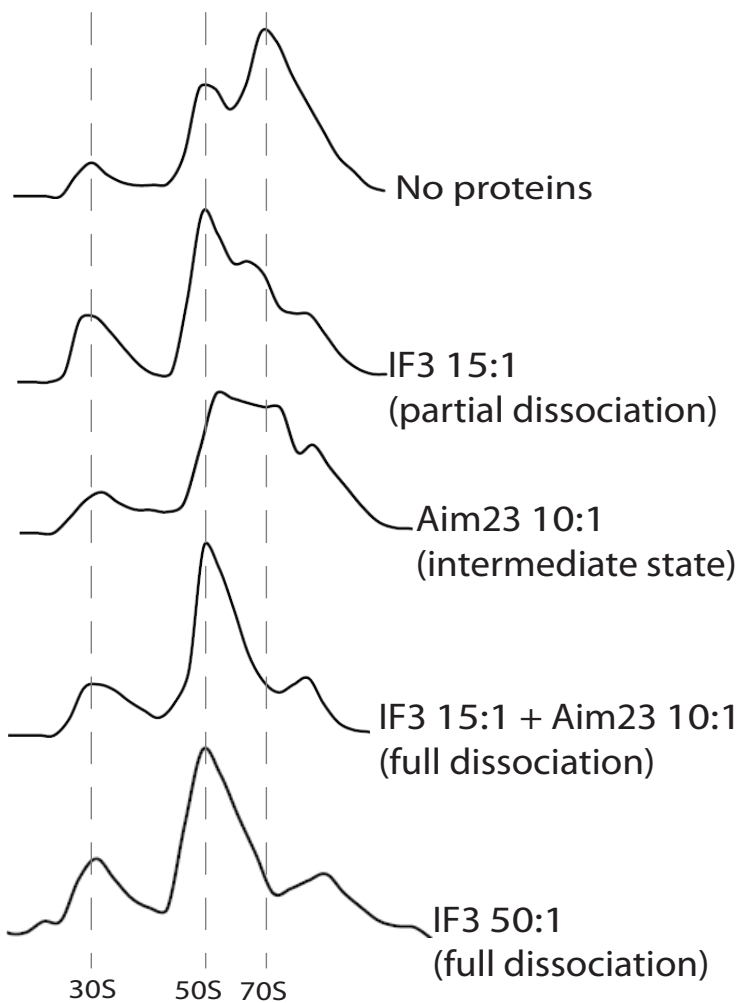
A.



B.



C.



D.

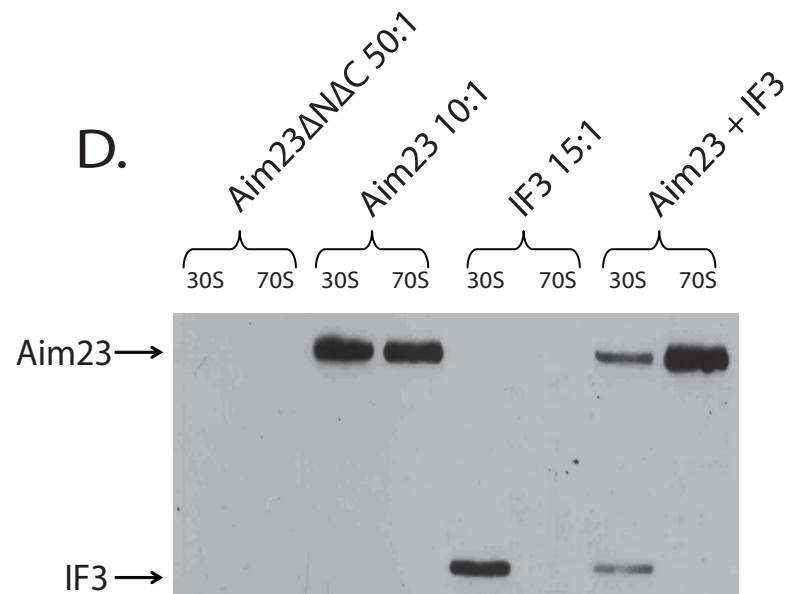


Figure 3

Model of Aim23p interactions with *E.coli* 16S RNA.

N-terminal extension is in light-pink, N-terminal domain is in hot-pink, C-terminal domain is in magenta and C-terminal extension is in deep-purple. 16S RNA is in black and white. **(A)** Overview of Aim23p location on 16S RNA. **(B)** Close-up view in same orientation. **(C)** Close-up view with counterclockwise rotation around vertical axis displaying proximity of N-terminal extension, C-terminal domain and 16S RNA.

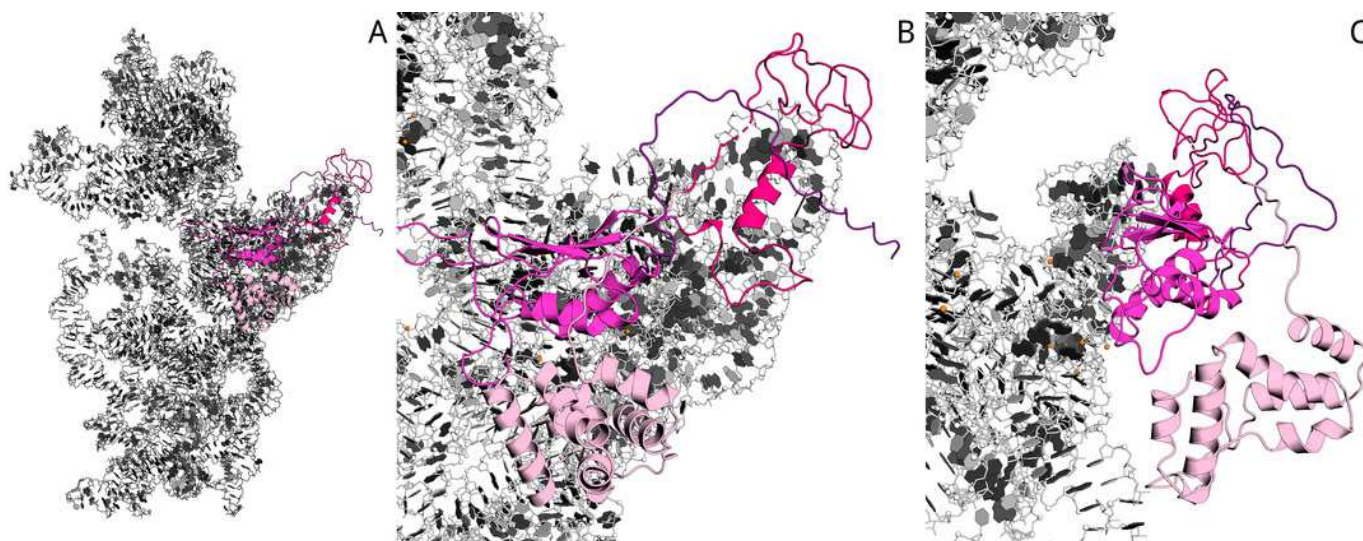


Figure 4(on next page)

The hypothetical scheme of the formation and dissociation of *E.coli* ribosomes intermediate state *in vitro*.

1. Initially, the small (SSU) and large (LSU) subunits of the ribosome are associated one to another (70S). Adding of Aim23p (the terminal extensions are represented by black boxes) changes the ribosome conformation making the subunits more flexible relative to one another and allowing their reciprocal movements without full dissociation (60S). 2. This intermediate dissociation state cannot spontaneously dissociate to the subunits in presence of Aim23p. 3. Adding more Aim23p, however, shifts the dissociation reaction equilibrium which results in appearance of the free SSU and LSU (30S + 50S). 4. Full dissociation of the intermediate can also be reached by adding *E.coli* IF3 in amount insufficient for dissociation of 70S ribosomes.

